Journal of Population Therapeutics & Clinical Pharmacology

RESEARCH ARTICLE
DOI: 10.53555/jptcp.v31i7.6864

ENHANCED DYE DEGRADATION USING TITANIUM DIOXIDE-MANGO SEED COMPOSITES: A NOVEL APPROACH TO PHOTOCATALYSIS

Iftikhar Ahmad Khan[1], Dr. Rehana Masood[2*], Fatima Mujahid[3], Dr Haseeb Umar[4], Saba Nosheen[5], Farzana Shaheen[6]

[1]Ph.D Scholar, Institute of Chemical Science, Gomal University Dera Ismail Khan, KP, Pakistan
[2*]Assistant Professor, Department of Biochemistry, Shaheed Benazir Bhutto Women University Peshawar, Pakistan
[3]Department of Chemistry, University of Agriculture Faisalabad, Pakistan,
[4]Department of Forensic Medicine, Alnafees Medical College, Isra University, Islamabad, Pakistan
[5]Department of Chemistry, Riphah International University Islamabad
[6]Lecturer, Department of Chemistry, Allama Iqbal Open University Islamabad, Pakistan

***Corresponding Author:** Dr. Rehana Masood
*Assistant Professor, Department of Biochemistry, Shaheed Benazir Bhutto Women University Peshawar, Pakistan

ABSTRACT:

Background: Titanium dioxide (TiO_2) is widely recognized for its effectiveness in photocatalysis, especially in environmental applications such as dye degradation. Despite its capabilities, TiO_2's performance can be limited by factors such as charge recombination and limited light absorption, necessitating modifications to improve its efficacy.

Objectives: This study aims to enhance the photocatalytic performance of TiO_2 by creating composites with mango seed powder. We investigate the photocatalytic degradation capabilities of these composites for two common dyes: crystal violet and methyl orange.

Methods: TiO_2 was mixed with mango seed powder in ratios of 1:1 (coded as S-A) and 1:2 (coded as S-B), followed by calcination at 500°C with a ramp of 10°C min^{-1} under a nitrogen flow. The photocatalytic activities of the composites were evaluated by measuring the degradation of crystal violet (100 mg L^{-1}) and methyl orange (50 mg L^{-1}) under light exposure for 90 minutes.

Results: The photocatalytic tests revealed that both composites efficiently degraded the dyes. Sample S-A achieved decolourization ratios of 83% for crystal violet and 96% for methyl orange, whereas sample S-B showed slightly lower efficiencies with 82% and 87% decolourization for the respective dyes. Additionally, the composites demonstrated superior particle separation from solutions post-photocatalysis compared to pure TiO_2.

Conclusion: Introducing mango seed powder into TiO_2 composites significantly enhanced their photocatalytic performance against both tested dyes. The observed improvement suggests that such composites are promising materials for the heterogeneous photocatalysis of dyes, providing a sustainable approach to wastewater treatment by utilizing agricultural waste products.

KEYWORDS: Titanium dioxide, Mango seed, Photocatalysis, Dye degradation, Composite materials

INTRODUCTION:

Many studies have been done on heterogeneous photocatalysis in treating wastewater, like textile dyes and hospital drugs. In photocatalytic processes, inorganic semiconductors like tungsten trioxide (WO3), zinc sulfide (ZnS), and iron III oxide (Fe2O3) are used a lot. However, titanium dioxide (TiO2) is one of the most popular photocatalysts because it is stable in physics, chemicals, and living things, cheap, not toxic, and very good at catalyzing reactions. Some things, like how hard it is to separate the fragments from the solution following the process, make them less useful (S. Das, Bhattacharya, & Das, 2024; Liza et al., 2024).

For example, the band gap energy of 3.2 eV makes it hard to use them in the visible range and makes it easy for the e-/h+ pair to recombine. The photocatalytic treatment of effluents needs catalysts that have high photocatalytic activity, make it easy for radicals to form that break down the organic pollutant, and are easy to separate from the solution that needs to be treated. This saves money on a second step in the process and lets them be used again.

Adding titanium dioxide to a carbonaceous matrix made from biomass, like mango seeds, is another way to improve its use. This can help increase the worth of the waste that is left over after heat treatment (Mahato, Singh, & Srivastava, 2024; Olowonyo, Salam, Aremu, & Lateef, 2024; Zhang, Zhang, Mujumdar, & Guo, 2024).

Heterogeneous Photocatalysis in Wastewater Treatment Studies

Study Reference	Photocatalyst(s) Used	Challenges Identified	Innovations in Photocatalyst Application	Examples of Application
S. Das, Bhattacharya, & Das, 2024	WO3, ZnS, Fe2O3, TiO2	Difficulty in separating photocatalyst post-process	-	-
Liza et al., 2024	TiO2	Low activity under visible light, recombination of e-/h+ pairs	-	-
Mahato, Singh, & Srivastava, 2024	TiO2, biomass carbon matrix	-	Use of mango seeds in a carbonaceous matrix to improve photocatalyst	-
Olowonyo, Salam, Aremu, & Lateef, 2024	TiO2, biomass carbon matrix	-	Enhancement of photocatalyst value through the use of biomass	-
Zhang, Zhang, Mujumdar, & Guo, 2024	TiO2, biomass carbon matrix	-	New composite materials from biomass waste and TiO2	-
El-Salamony et al., 2024	TiO2, sugarcane bagasse	Complexity of the production process	Nanocomposites using sugarcane bagasse	Photocatalysis of methylene blue using visible light
Azeroual et al., 2024	TiO2, mango seeds	-	Heating of TiO2 with mango seeds in varying ratios	Photocatalysis using crystal violet dyes
Jadon, Kour, Bhat, & Sharma, 2024	TiO2, mango seeds	-	Optimization of composite ratios for enhanced photocatalytic activity	Photocatalysis using methyl orange
Taghizadeh-Lendeh et al., 2024	TiO2, mango seeds	Lack of research on particle separation post-process	-	-

Through this process, a new material called a composite can be made. This type of material has qualities that aren't found in any materials that make it up. In this way of thinking, the work of El-Salamony et al. demonstrated promising results in the photocatalysis of methylene blue using visible light and nanocomposites made from sugarcane bagasse and titanium dioxide. However, the steps needed to make this material are complicated, and no one has looked into how to separate the particles from the solution at the final stage of the process. This is in contrast to industrial titanium dioxide. Because of this, we present a plan to make a new material by heating commercial titanium dioxide and mango seeds in 1:1 and 1:2 ratios. We will test the photocatalytic properties of this material utilizing crystal violet dyes and methyl orange as examples (Azeroual et al., 2024; Jadon, Kour, Bhat, & Sharma, 2024; Taghizadeh-Lendeh, Sarrafi, Alihosseini, & Bahri-Laleh, 2024).

MATERIALS AND METHODS:

COMPOSITE PREPARATION:

The composites were made from industrial titanium dioxide Degussa P-25 and mango seeds mixed in equal parts (1:1). The precursors were put into a jar with pure water, and the temperature was kept below 30°C. In contrast, the water was magnetically stirred for 12 hours. The collected solids were filtered and processed at 70 ºC for 72 hours. They were given the names SS1 and SS2. After that, the mixtures were heated in a Ney-Vulcan muffle furnace, 3-550PD, with a heating rate of 10 ºC min-1 and a nitrogen flow rate of 80 mL min-1. The temperature was 500°C for 2 hours, and the finished samples were labelled S-A (1:1) and S-B (1:2). Figure 1 shows the steps that were taken to get ready (Khalid et al., 2024; Shan et al., 2024; Suciyati, Manurung, Junaidi, & Situmeang).

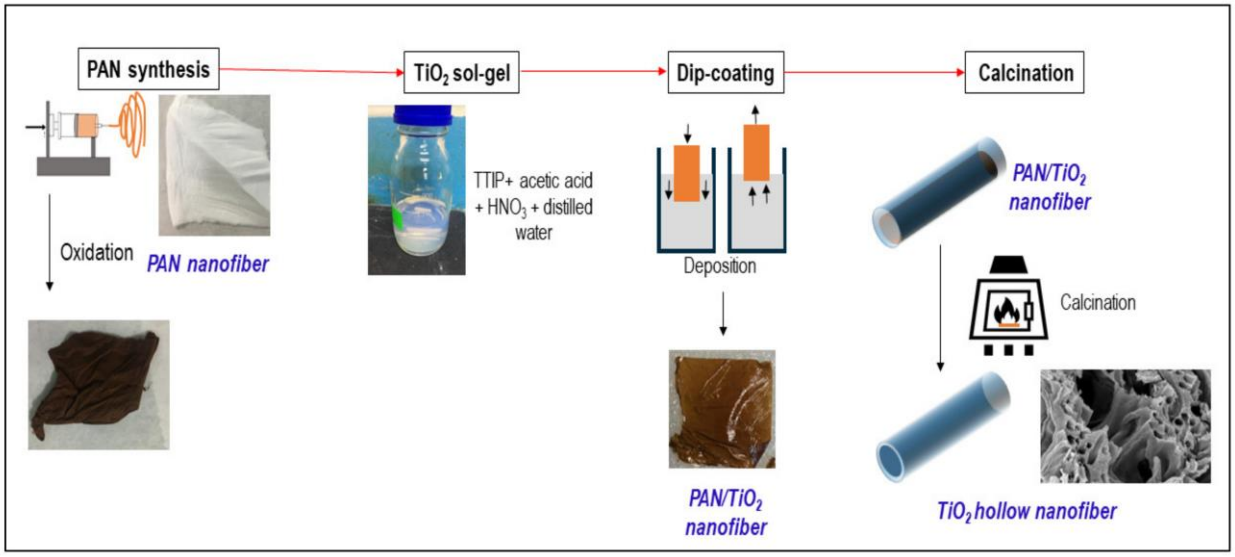

Figure 1. Steps to obtain S-A and S-B samples

DESCRIPTION:

X-RAY DIFFRACTOMETRY (XRD):

Used a Shimadzu diffractometer (model XRD 6000) with CuKα radiation (λ = 1.5418 A) and 40 KV and 30 µA tube voltage and current to do X-ray diffraction (XRD) analyses. With a step size of 2° min-1 and 0.6 sec step-1, the 2θ scan was done from 10° to 80° (Mohamed, Yılmaz, Güner, & El Nemr, 2024).

FOURIER TRANSFORM INFRARED (FTIR) SPECTROSCOPY

Molecular absorption spectroscopy in the Fourier transformation of infrared (FTIR) region was carried out on a Perkin Elmer Spectrum 100 machine. The sample was mixed with KBr and then pressed to make a tablet at room temperature. The spectra were taken in the range of 4000 to 400 cm-1, with a precision of 4 cm-1 (Sah, Gite, Sonawane, & Raut, 2024).

SPECIFIC SURFACE MEASUREMENT:
The BET method and Quantachrome Instruments version 11.03 tools measured specific surface areas. Five milligrams of samples were weighed out, and they were heated in three stages. The first stage heated the samples to 373 K for 15 minutes. The second stage heated them to 473 K for 15 minutes, and the third stage heated them until they reached 623 K for 30 minutes (Alshammari, 2024; Nian et al., 2024).

SCANNING ELECTRON MICROSCOPY (SEM):
SEM (scanning electron microscope) analyses were done in a JEOL scanning electron microscope room model T330 connected to a computer with special software.

TURBIDITY ANALYSIS:
The Baiana Water and Sanitation Company (EMBASA), based in Salvador Bahia, Brazil, evaluated the turbidity of the crystal violet (CV) solution from the photocatalytic test. This was done per the Ministry of Health's consolidation ordinance (Flores-Contreras et al., 2024).

PHOTOCATALYTIC TESTS:
In the photocatalytic tests, 100 mg L-1 of CV dye and 50 mg L-1 of AlaM were mixed. The tests were done in a photoreactor that was made at home. It had a mercury vapour lamp (125 W) and a jacket. Mixed amounts of 0.2 g were used for AlaM photocatalysis and 0.3 g for CV photocatalysis. At first, the system was stirred for 30 minutes while it was dark. The lamp was turned on once this time was up, and the aliquots were taken out every 5 to 90 minutes. A Perkin Elmer UV-VIS spectrophotometer, model Lambda 35, was used to look at the materials at 589 nm for the CV and 460 nm for the AlaM. The tests were done without the catalyst so that they could be compared (photolysis) (Bansal, Singh, Sharma, Sundaramurthy, & Mehta, 2024; Eswaran et al., 2024; Wahab et al., 2024).

RESULTS AND DISCUSSION:
X-RAY DIFFRACTOMETRY:
The crystallographic profiles of the composites (S-A and S-B) and industrial titanium dioxide can be seen in Figure 2. References taken from a database were used to compare the results. Anatase and rutile phases with high crystallinity can be seen in the P25 samples of titanium dioxide and its compounds (Rameez, Khan, Ahmad, & Ahmad, 2024).

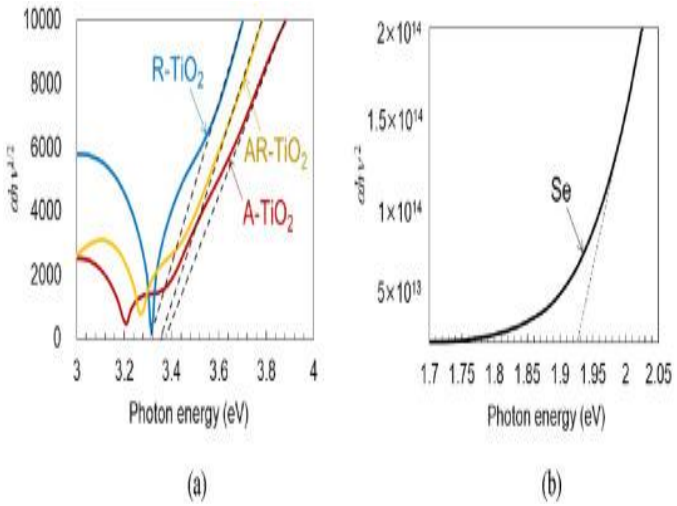

Figure 2. Crystallographic profiles of composites S-A and S-B and commercial TiO2

The Bragg reflections of commercial titanium dioxide and alloys were found at 2θ = 25,350, 37,810, 48,070, 54,040, 55,210, 68,830, 70,390, and 75.03. These points correspond to the anatase phase of titanium oxide and are in excellent accordance with references (JCPDS 89-4921). TiO2 and its mixtures have diffraction peaks at 2θ = 27.38°, 35.99°, 41.27°, 56.55°, and 62.72°, which show that the phase known as rutile is also found (Kenda et al., 2024; Murugappan, Pebam, Sankaranarayanan, & Rengan, 2024).

Based on the crystallographic profiles (Figure 2), we can see that the peaks in the TiO2 and composite profiles are the same. This means that the production methods have kept the oxide's crystalline structure in the carbon matrix (Rout & Pradhan, 2024).

INFRARED WITH FOURIER TRANSFORMS (FTIR):

The spectrum of the two compounds (Figure 3) shows wide bands around 3500 cm-1. These are caused by the hydroxyl groups (OH) stretching vibrations, which come from the water attached to the material's surface. Around 1635 cm-1, vibration bands are seen caused by the bends of the –OH groups of the alcohols in the benzene ring. These bands may be linked to the presence of lignin. The bands that lie around 1385 cm-1 are connected to the carbonyl group and the C–O bond (Rahman, Daniel, & Uahengo, 2024; Sani, Khezerlou, Tavassoli, Abedini, & McClements, 2024).

The bands that absorb light between 460 and 750 cm-1 are caused by the vibrations of the links between Ti and O and Ti, and O. The bands between 1000 and 1300 cm-1 are somewhat more noticeable on the S-B sample's curve. On the other hand, the bands seen between 460 and 750 cm-1 are more clearly defined on the S-A sample's curve. It concerns the amount of titanium dioxide to biomass in composites (Din, Rehman, Hussain, & Khalid, 2024; Meziane et al., 2024).

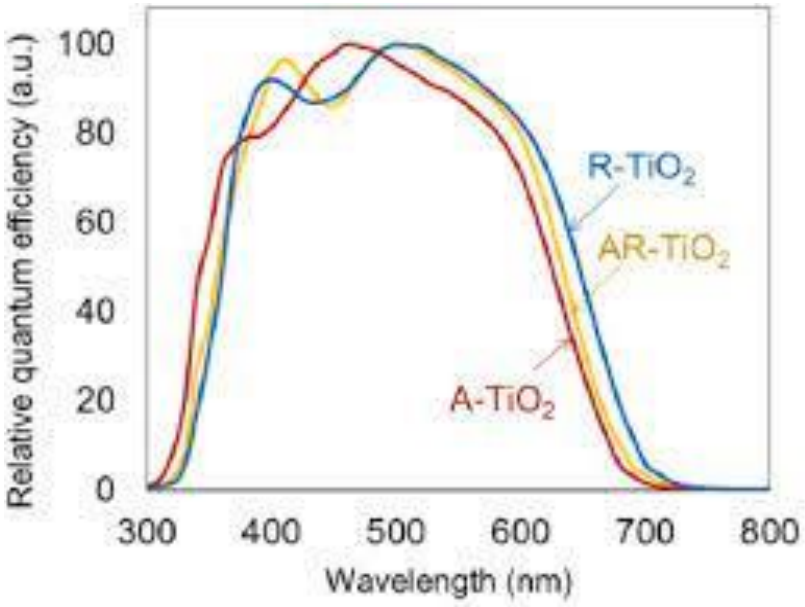

Figure 3. Fourier transform infrared of the S-A and S-B composites

SPECIFIC AREA:

The specific surface area of sample S-B was greater than that of sample S-A, as shown in Table 1. This result shows that adding more mango seeds to the mixture causes more gas to be released during the heating process, which in turn causes more free volume to be created in the solid as the gases escape (de Menezes, de Lima Leite, Dos Santos, Aria, & Aroucha, 2024).

Table 1. Specific surface area of composites S-A and S-B

Sample	Area (M2 G-1)
S-B	108
S-A	91

SCANNING ELECTRON MICROSCOPY (SEM):
SEM STANDS FOR SCANNING ELECTRON MICROSCOPY:
The micrographs show that when the amount of titanium dioxide and biomass is changed from 1:1 to 1:2, there is a significant change in the shape of the particles and how they are spread out in the carbon matrix (Figures 4 and 5) (Taghipour, Nia, Hokmabadi, & Yahia, 2024).

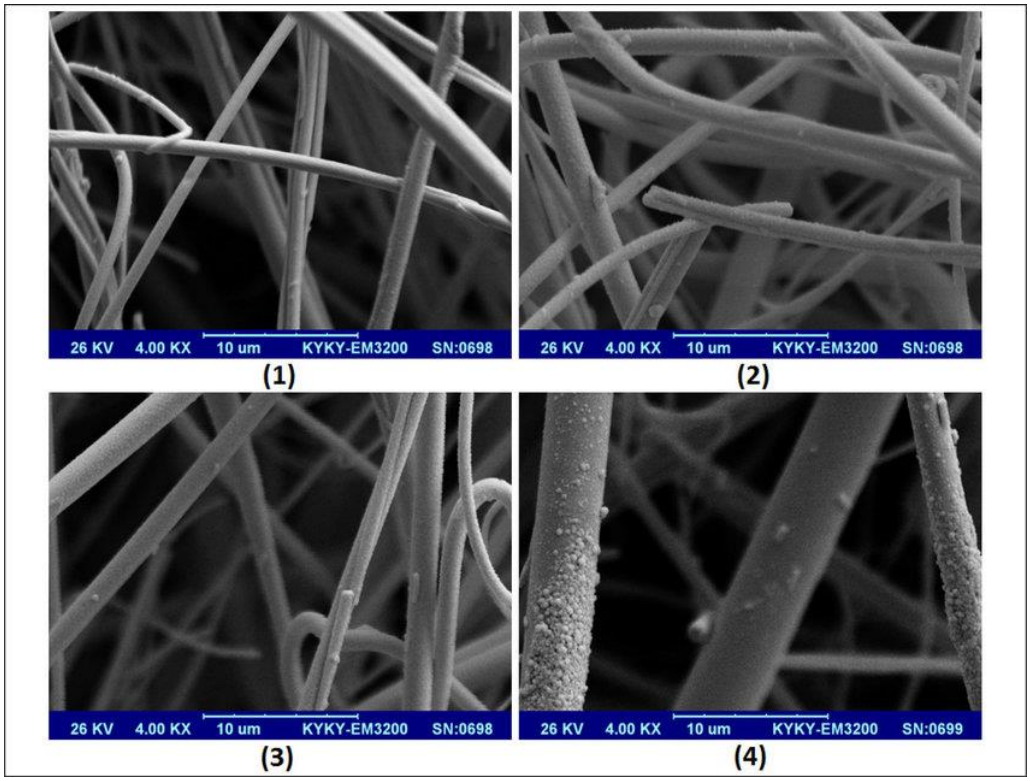

Figure 4. Scanning electron microscopy of the S-A composite

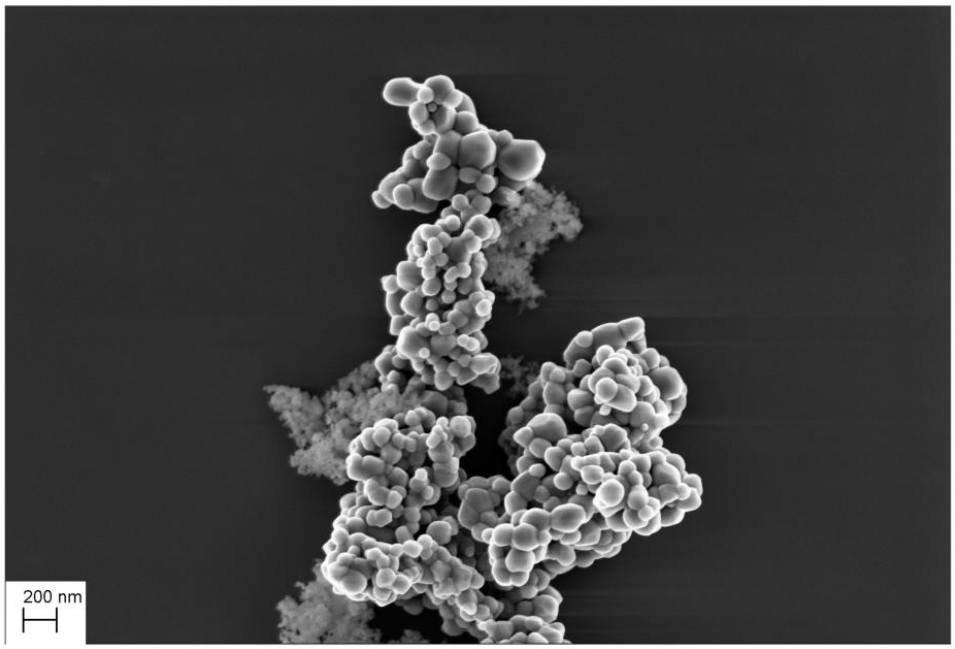

Figure 5. Scanning electron microscopy of S-B composite

PHOTOCATALYTIC TESTS:

Because of photocatalysis, mixtures of crystal violet (CV) and methyl orange (AlaM) dyes changed colour, as shown in Figures 6 and 7.

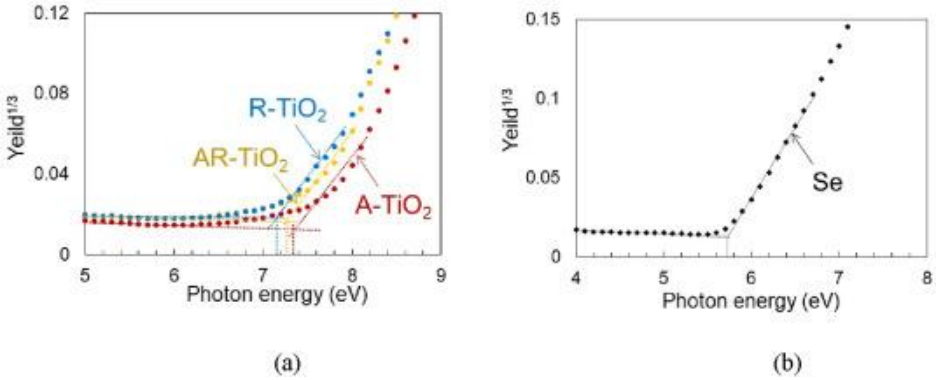

Figure 6. Crystal Violet photocatalysis

After 90 minutes, there wasn't a significant change in how well the samples worked in CV photocatalysis (S-A 83% vs. S-B 82%), but it was a little better than commercial TiO2 (79%). The S-A composite removed 96% of the methyl orange colour after 90 minutes, which was better than the S-B composite, which only removed 86 and 87%, respectively, which was about the same as commercial titanium dioxide (Siddiqui et al., 2024; Tabassum et al., 2024).

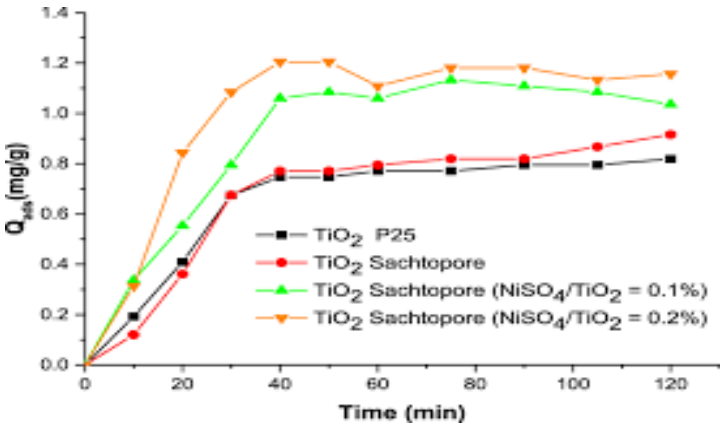

Figure 7. Methyl orange photocatalysis

Blends are much better for post-process separation because the solids (S-A and S-B) settle more quickly than commercial titanium dioxide. This can be seen through the comparison of images B and C (Figure 8) and 9 and 10 (Figure 9) (Bharti et al., 2024).

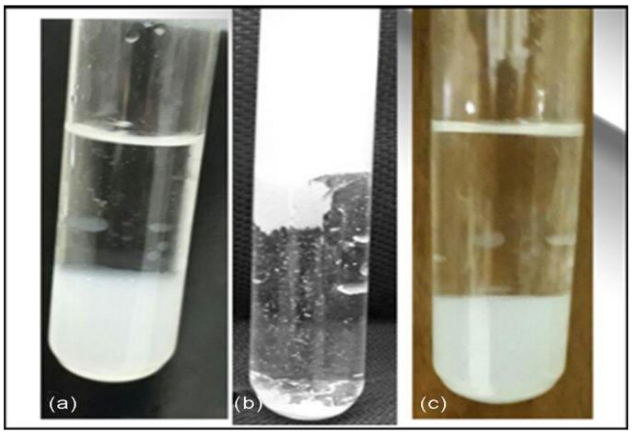

Figure 8. CV solutions: initial (A), following photocatalysis: with composites (B) with TiO2 (C)

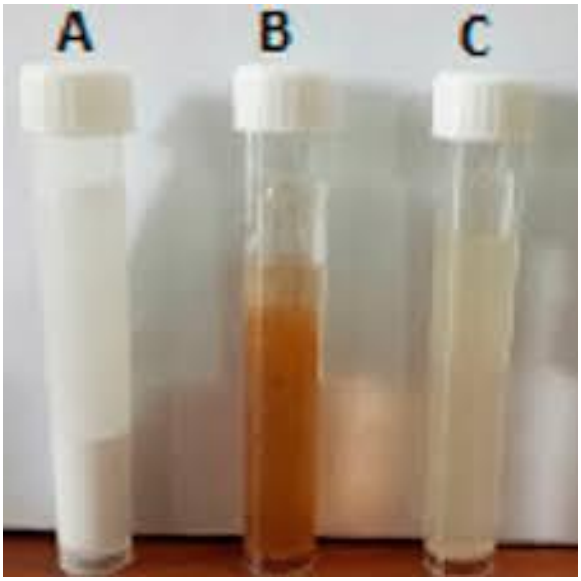

Figure 9. AM solutions: initial (0), after photocatalysis with composites (9) and TiO2 (10)

Because of this, solutions made with titanium dioxide photocatalysis are cloudier than solutions made with composites. This part concerns how much semiconductor is left over after spinning. The TiO2 is not fully poured; some are mixed in with the solution, and a small amount stays on the container wall. In this case, there would need to be a second separation step (Mazibuko, Onwubu, Thabang, & Mdluli, 2024; Narwal et al., 2024).

This result is also supported by the work of Borges et al. and the comments of Ribeiro et al., who used TiO2 to do photodegradation tests on the wastewater from washing jeans. This showed them that the solid was still spread out in the medium after 24 hours. The samples were synthesized fully, so there is no need for an extra step to ensure that the semiconductors are sunk into the dye solution (Gupta et al.; Petcu et al., 2024).

TURBIDITY:

After titanium dioxide and light tests, the CV solution had 2,500 turbidity units (UT). The CV solution with the synthesized compounds had a turbidity of 0.65 UT because of photocatalysis. These quantitative results back up the qualitative ones because, even after centrifugation, the significant turbidity of the solution that still shows scattered TiO2 is seen (Figure 9 C). The Ministry of Health says that 5 UT is the lowest turbidity water level and is still considered safe for people to drink. Because of this, the photocatalytic process that uses the synthesized compounds is better than the one that uses Degussa TiO2 P-25 (D. Das, Verma, & Tangjang, 2024).

CONCLUSION:

When titanium dioxide is mixed with carbonaceous material, it doesn't change the structure of the oxide itself. However, the specific region's values and morphological features are different when the titanium dioxide to mango seed ratio is 1:1 or 1:2. Compared to commercial TiO2, using composites keeps or slightly boosts the colour change of the dyes in photocatalysis after 90 minutes. This is true for both crystal violet and methyl orange. Both combinations solidified better after the process, which made separation easier. This means these materials can be used in photocatalysis without undergoing another separation step. So, the titanium dioxide/carbonaceous material compounds made are valuable alternatives for the heterogeneous photocatalysis of dyes.

REFERENCES:

1. Alshammari, A. (2024). Impact of lignocellulosic biomass-derived graphene-titanium oxide nanocomposite as an electrode for sustainable performance in microbial fuel cell. International Journal of Environmental Science and Technology, 21(5), 5185-5202.

2. Azeroual, S., Khatib, K., Belfkira, A., Ablouh, E.-H., Hanani, Z., Taourirte, M., & Jalal, R. (2024). A novel approach for adsorption of organic dyes from aqueous solutions using a sodium alginate/titanium dioxide nanowire doped with zirconium cryogel beads. Frontiers in Chemistry, 12, 1285230.
3. Bansal, H., Singh, S., Sharma, A., Sundaramurthy, S., & Mehta, S. (2024). Polymer nanocomposite films and coatings for antimicrobial and antifungal applications Polymer Nanocomposite Films and Coatings (pp. 785-815): Elsevier.
4. Bharti, A. S., Baran, C., Bhardwaj, A. K., Tripathi, S., Pandey, R., & Uttam, K. N. (2024). Domestic waste utilization in synthesizing functional nanomaterial Green and Sustainable Approaches Using Wastes for the Production of Multifunctional Nanomaterials (pp. 61-76): Elsevier.
5. Das, D., Verma, K., & Tangjang, S. (2024). A Comprehensive Perspective of Conventional and Biogenic Nanoparticles Biogenic Nanomaterial for Health and Environment (pp. 1-17): CRC Press.
6. Das, S., Bhattacharya, S., & Das, P. (2024). Titanium oxide–coated coconut husk–derived biochar composite and its application to remove crystal violet dye. Biomass Conversion and Biorefinery, 14(4), 5035-5051.
7. de Menezes, F. L. G., de Lima Leite, R. H., Dos Santos, F. K. G., Aria, A. I., & Aroucha, E. M. M. (2024). TiO2 incorporated into a blend of biopolymeric matrices improves film properties and affects the postharvest conservation of papaya fruits under UV light. Food Chemistry, 433, 137387.
8. Din, M. I., Rehman, S., Hussain, Z., & Khalid, R. (2024). Green synthesis of strontium oxide nanoparticles and strontium based nanocomposites prepared by plant extract: a critical review. Reviews in Inorganic Chemistry, 44(1), 91-116.
9. Eswaran, S. G., Stalin, T., Thiruppathi, D., Madhu, M., Santhoshkumar, S., Warchol, J., . . . Vasimalai, N. (2024). One-pot synthesis of carbon dots from neem resin, selective detection of Fe (ii) ions, and photocatalytic degradation of toxic dyes. RSC Sustainability.
10. Flores-Contreras, E. A., González-González, R. B., Pablo Pizaña-Aranda, J. J., Parra-Arroyo, L., Rodríguez-Aguayo, A. A., Iñiguez-Moreno, M., . . . Parra-Saldívar, R. (2024). Agricultural waste is a sustainable source for nanoparticle synthesis, and its antimicrobial properties are helpful for food preservation. Frontiers in Nanotechnology, 6, 1346069.
11. Gupta, R. K., Abd El Gawad, F., Ali, E. A., Karunanithi, S., Yugiani, P., & Srivastav, P. P. Measurement: Food.
12. Jadon, N., Kour, B., Bhat, B. A., & Sharma, H. K. (2024). Green Synthesis Derived Novel Fe2O3/ZnO Nanocomposite for Efficient Photocatalytic Degradation of Methyl Orange Dye. Current Analytical Chemistry, 20(3), 162-174.
13. Kenda, G. T., Fotsop, C. G., Tchuifon, D. R. T., Kouteu, P. A. N., Fanle, T. F., & Anagho, S. G. (2024). Building TiO2-doped magnetic biochars from Citrus Sinensis Peels as low-cost materials for improved dye degradation using a mathematical approach. Applied Surface Science Advances, 19, 100554.
14. Khalid, S., Hassan, S. A., Javaid, H., Zahid, M., Naeem, M., Bhat, Z. F., . . . Aadil, R. M. (2024). Factors responsible for spoilage, drawbacks of conventional packaging, and advanced packaging systems for tomatoes. Journal of Agriculture and Food Research, 100962.
15. Liza, T. Z., Tusher, M. M. H., Anwar, F., Monika, M. F., Amin, K. F., & Asrafuzzaman, F. (2024). Effect of Ag-doping on morphology, structure, band gap, and photocatalytic activity of bio-mediated TiO2 nanoparticles. Results in Materials, 22, 100559.
16. Mahato, R. P., Singh, P., & Srivastava, S. (2024). Prospects and Challenges of Nanofilms-based Edible Food Coatings for Enhancement of Their Shelf Life. The Nanotechnology Driven Agriculture, 204-224.
17. Mazibuko, M. T., Onwubu, S. C., Thabang, M. H., & Mdluli, P. S. (2024). Unlocking Heavy Metal Remediation Potential: A Review of Cellulose-Silica Composites.

18. Meziane, H., Laita, M., Azzaoui, K., Boulouiz, A., Neffa, M., Sabbahi, R., . . . Siaj, M. (2024). Nanocellulose fibres: A review of preparation methods, characterization techniques, and reinforcement applications. Moroccan Journal of Chemistry, 12(1), 12-11 (2024) 2305-2343.
19. Mohamed, S. M. I., Yılmaz, M., Güner, E. K., & El Nemr, A. (2024). Synthesis and characterization of iron oxide-commercial activated carbon nanocomposite to remove hexavalent chromium (Cr6+) ions and Mordant Violet 40 (MV40) dye. Scientific Reports, 14(1), 1241.
20. Murugappan, S., Pebam, M., Sankaranarayanan, S. A., & Rengan, A. K. (2024). Drug-delivery, Antimicrobial, Anticancerous Applications of Green Synthesized Nanomaterials. Green Synthesis of Nanomaterials: Biological and Environmental Applications, 131-168.
21. Narwal, N., Katyal, D., Malik, A., Kataria, N., Bhardwaj, A. K., Rakib, M. R. J., & Kakakhel, M. A. (2024). Sustainable advances in the synthesis of waste-derived value-added metal nanoparticles and their applications Green and Sustainable Approaches Using Wastes for the Production of Multifunctional Nanomaterials (pp. 17-33): Elsevier.
22. Nian, L., Wang, M., Sun, X., Zeng, Y., Xie, Y., Cheng, S., & Cao, C. (2024). Biodegradable active packaging: Components, preparation, and applications in preserving postharvest perishable fruits and vegetables. Critical Reviews in Food Science and Nutrition, 64(8), 2304-2339.
23. Olowonyo, I. A., Salam, K. K., Aremu, M. O., & Lateef, A. (2024). Synthesis, characterization, and adsorptive performance of titanium dioxide nanoparticles modified groundnut shell activated carbon on ibuprofen removal from pharmaceutical wastewater. Waste Management Bulletin, 1(4), 217-233.
24. Petcu, G., Ciobanu, E. M., Paun, G., Neagu, E., Baran, A., Trica, B., . . . Badaluta, A. (2024). Hybrid Materials Obtained by Immobilization of Biosynthesized Ag Nanoparticles with Antioxidant and Antimicrobial Activity. International Journal of Molecular Sciences, 25(7), 4003.
25. Rahman, A., Daniel, L. S., & Uahengo, V. (2024). Iron Oxide Nanomaterials for Water Purification.
26. Rameez, M., Khan, N., Ahmad, S., & Ahmad, M. M. (2024). Bionanocomposites: A new approach for fungal disease management. Biocatalysis and Agricultural Biotechnology, 103115.
27. Rout, S. S., & Pradhan, K. C. (2024). A review on antimicrobial nano-based edible packaging: Sustainable applications and emerging trends in the food industry. Food Control, 110470.
28. Sah, P. M., Gite, S. G., Sonawane, R., & Raut, R. W. (2024). Biogenic Nanomaterials as a Catalyst for Photocatalytic Dye Degradation Biogenic Nanomaterials for Environmental Sustainability: Principles, Practices, and Opportunities (pp. 409-433): Springer.
29. Sani, M. A., Khezerlou, A., Tavassoli, M., Abedini, A. H., & McClements, D. J. (2024). Development of sustainable UV-screening food packaging materials: A review of recent advances. Trends in Food Science & Technology, 104366.
30. Shan, A., Baig, M. M., Kamran, U., Jamal, H., Arif, M. U., Hassan, M., . . . Lee, S. G. (2024). New Y0. 045Ni0. 045Fe2. 91O4 nanowires decorated over mesoporous silica for crystal violet removal: Response surface methodology optimization, kinetics, and isothermal studies. Ceramics International.
31. Siddiqui, S. A., Yang, X., Deshmukh, R. K., Gaikwad, K. K., Bahmid, N. A., & Castro-Muñoz, R. (2024). Recent advances in reinforced bioplastics for food packaging–A critical review. International Journal of Biological Macromolecules, 130399.
32. Suciyati, S. W., Manurung, P., Junaidi, J., & Situmeang, R. Optical and Crystal Structure Properties of ZnO Nanoparticle Synthesized through Biosynthesis Method for Photocatalysis Application. Indonesian Journal of Chemistry.
33. Tabassum, N., Rafique, U., Qayyum, M., Mohammed, A. A., Asif, S., & Bokhari, A. (2024). Kaolin–Polyvinyl Alcohol–Potato Starch Composite Films for Environmentally Friendly Packaging: Optimization and Characterization. Journal of Composites Science, 8(1), 29.

34. Taghipour, S., Nia, A. E., Hokmabadi, H., & Yahia, E. M. (2024). Quality evaluation of fresh pistachios (Pistacia vera L.) cultivars coated with chitosan/TiO2 nanocomposite. International Journal of Biological Macromolecules, 258, 129055.
35. Taghizadeh-Lendeh, P., Sarrafi, A. H. M., Alihosseini, A., & Bahri-Laleh, N. (2024). Synthesis and characterization of ZnO/TiO2 incorporated activated carbon as photocatalyst for gas refinery effluent treatment. Polyhedron, 247, 116715.
36. Wahab, A., Muhammad, M., Ullah, S., Abdi, G., Shah, G. M., Zaman, W., & Ayaz, A. (2024). Agriculture and environmental management through nanotechnology: Eco-friendly nanomaterial synthesis for soil-plant systems, food safety, and sustainability. Science of The Total Environment, 171862.
37. Zhang, L., Zhang, M., Mujumdar, A. S., & Guo, Z. (2024). Preparation and characterization of TiO2 photocatalyst films and their application for preservation of Agaricus bisporus in combination with blue-violet LEDs. Food Bioscience, 59, 103860.